Ergodicity Breaking and Deviation from Eigenstate Thermalization in Relativistic Quantum Field Theory

Miha Srdinšek,[1,2,3,*] Tomaž Prosen,[4] and Spyros Sotiriadis[5,6]

[1]Institut des Sciences du Calcul et des Données (ISCD), Sorbonne Université, 4 Place Jussieu, 75005 Paris, France
[2]Institut de Minéralogie, de Physique des Matériaux et de Cosmochimie (IMPMC), Sorbonne Université, CNRS UMR 7590, MNHM, 4 Place Jussieu, 75005 Paris, France
[3]Processus d'Activation Sélectif par Transfert d'Energie Uni-électronique ou Radiative (PASTEUR), CNRS UMR 8640, Département de Chimie, École Normale Superieure, 24 rue Lhomond, 75005 Paris, France
[4]Faculty of Mathematics and Physics, University of Ljubljana, Jadranska 19, SI-1000 Ljubljana, Slovenia
[5]Institute of Theoretical and Computational Physics, Department of Physics, University of Crete, 71003 Heraklion, Greece
[6]Dahlem Center for Complex Quantum Systems, Freie Universität Berlin, 14195 Berlin, Germany

(Received 11 May 2023; revised 10 October 2023; accepted 1 December 2023; published 12 January 2024)

The validity of the ergodic hypothesis in quantum systems can be rephrased in the form of the eigenstate thermalization hypothesis (ETH), a set of statistical properties for the matrix elements of local observables in energy eigenstates, which is expected to hold in any ergodic system. We test the ETH in a nonintegrable model of relativistic quantum field theory (QFT) using the numerical method of Hamiltonian truncation in combination with analytical arguments based on Lorentz symmetry and renormalization group theory. We find that there is an infinite sequence of eigenstates with the characteristics of quantum many-body scars—that is, exceptional eigenstates with observable expectation values that lie far from thermal values—and we show that these states are one-quasiparticle states. We argue that in the thermodynamic limit the eigenstates cover the entire area between two diverging lines: the line of one-quasiparticle states, whose direction is dictated by relativistic kinematics, and the thermal average line. Our results suggest that the strong version of the ETH is violated in any relativistic QFT whose spectrum admits a quasiparticle description.

DOI: 10.1103/PhysRevLett.132.021601

Introduction.—One of the main theoretical concepts for understanding and testing ergodicity in quantum systems is the eigenstate thermalization hypothesis (ETH) [1,2], which states that in a chaotic quantum system—to be termed ergodic—the expectation values of a local observable in generic high-energy eigenstates concentrate at the corresponding thermal expectation values as we approach the thermodynamic limit. The validity of the ETH in quantum many-body systems has been studied and verified numerically in a large number of nonintegrable lattice models [3–11], even though exceptions to this rule do exist, at least in a weak sense. For instance, in models exhibiting so-called *quantum many-body scars* (QMBS) [12–30], expectation values of local observables are anomalously distant from the corresponding thermal values for an infinite sequence—yet of measure zero—of eigenstates. Whenever such atypical states are present, the crucial question that arises is what happens in the thermodynamic limit: Do these states vanish (strong ETH), do they persist but correspond to a zero measure subset of the spectrum (weak ETH), or do they correspond to a finite density? Only the strong version of the ETH can guarantee thermalization [31].

A class of quantum many-body models that remains largely unexplored in this respect is that of nonintegrable quantum field theories (QFTs), i.e., relativistic models of quantum fields, which constitute the theoretical basis of particle physics and adjacent research areas. QFT models are defined over Hilbert spaces of infinite dimension, for which reason the numerical study of their spectra is inevitably approximate and remains an especially challenging task. Some pioneering studies of the validity of the ETH in QFT have focused on conformal field theories (CFTs) [32–39], which exhibit quantum chaotic characteristics in the limit of large central charge [40–47]. In a general nonintegrable QFT, numerical tests of the ETH can be performed using lattice discretization [48,49] or Hamiltonian truncation (HT) methods [50–52]. Studying a class of prototypical nonintegrable models of $(1+1)$D QFT based on HT, we have recently demonstrated that, although their level spacing statistics are consistent with random matrix theory predictions, the statistics of their eigenvector components is markedly different from that of random matrices [53]. The observation was further confirmed by Delacrétaz *et al.* 52]] for the case of the ϕ^4 model. Eigenvector statistics is strongly related to the validity of the ETH; therefore, our observation naturally raises the question of whether the ETH is satisfied in these models.

In this Letter, we argue that, unlike in typical lattice models, violations of the ETH are commonplace in a large class of nonintegrable QFTs. First, there are exceptional

eigenstates with QMBS characteristics. Similar special states have been observed also in other QFT models [50,52], and in one of them [50] their presence has been associated to confinement, resulting in the absence of thermalization after a quench [54]. Second, the eigenstates do not all concentrate close to a line in the thermodynamic limit, as prescribed by the ETH, but remain spread in a wide area, from an edge line where QMBS-like states are located to the thermal average line.

Our numerical results, based on HT applied to a nonintegrable QFT, demonstrate the existence of eigenstates that have QMBS characteristics [12,13]: They are outliers in ETH diagrams, span the entire energy range of the spectrum, are approximately equidistant in energy, and have low (Fourier-space) entanglement. In addition, the presence of such states turns out to persist as the system size or interaction strength increases, at least within the limits of applicability of our method.

One interpretation of QMBS is in terms of quasiparticle states at unusually high-energy scales in the spectrum [30]. We find that the scarlike states we observe can indeed be explained as quasiparticle states. Based on this interpretation, we show that their presence in the thermodynamic limit, at high energies, and for arbitrary interaction strength follows from relativistic kinematics, which at the same time means that they correspond to physically relevant quantum states.

On the other hand, based on renormalization group (RG) theory, it is expected that in the high-energy (ultraviolet) limit the thermal average line follows that of the CFT that describes the ultraviolet fixed point of the given model. This is because in this limit any RG relevant operator by definition reduces to only a weak perturbation of the CFT [55,56]. The asymptotic CFT thermal line generally diverges from the line corresponding to one-quasiparticle states, which means that eigenstates are expected to cover the entire area between them. Based on the above arguments, we conclude that deviations from ETH are expected in any Lorentz invariant relativistic QFT model whose spectrum admits a quasiparticle description.

Model and method.—We consider the *double sine-Gordon* (DSG) model [57–63], a nonintegrable $(1+1)$D bosonic QFT that is described by the Hamiltonian (in units $\hbar = c = 1$)

$$H_{\mathrm{DSG}} = H_0 - \lambda_1 V(\beta_1) - \lambda_2 V(\beta_2), \tag{1}$$

$$H_0 = \int_0^L :\left(\frac{1}{2}\Pi^2 + \frac{1}{2}(\partial_x \phi)^2\right): \mathrm{d}x, \tag{2}$$

$$V(\beta) = \int_0^L :\cos\beta\phi: \mathrm{d}x. \tag{3}$$

The low-energy spectrum of DSG can be studied efficiently using HT in the basis of the free massless boson model H_0 truncated by imposing a maximum energy cutoff [51,60,61]. This is an application of the truncated conformal space approach (TCSA) [64,65], where the unperturbed model is a CFT and the construction of the perturbation matrix is facilitated using the algebraic CFT toolkit. TCSA has been used to study spectral properties as well as equilibrium and quench dynamics in the sine-Gordon model and perturbations thereof [53,66–71]. The convergence of the numerically computed eigendecomposition for increasing cutoff is guaranteed for perturbations that are RG relevant operators and is faster when the scaling dimension of the perturbation is smaller, meaning that TCSA eigenstates can be used for testing the ETH [72]. The smaller the system size L, the interaction strength parameters λ_i, and frequencies β_i in Eq. (3), the faster the convergence.

Numerical results.—We study the spectrum of DSG for Dirichlet boundary conditions at $\beta_1 = 1$ and $\beta_2 = 2.5$ with equal mixing parameters $\lambda_1 = \lambda_2 = \lambda$, in which case the model is far from all integrable regimes. In particular, its level spacing statistics are consistent with random matrix theory predictions for any value of the interaction strength λ even in proximity to the CFT point [53]. At the same time, the spectrum converges up to sufficiently high energies and for interactions sufficiently far from the perturbative regime. The system size dependence of the operators H_0 and $V(\beta)$ in the free massless boson basis can be shown to be simply $H_0 \propto 1/L$ and $V(\beta) \propto L$, respectively, so it is convenient to compute the spectrum of the rescaled Hamiltonian $\tilde{H}_{\mathrm{DSG}} = \tilde{H}_0 - \lambda(L/\pi)^2[\tilde{V}(\beta_1) + \tilde{V}(\beta_2)]$, where $\tilde{H}_0 = H_0(L/\pi)$, whose energy eigenvalues are integers, and $\tilde{V}(\beta) = V(\beta)(\pi/L)$. This way, it is clear that there is only one free parameter, $\mu \equiv \lambda(L/\pi)^2$, and increasing the interaction coupling has essentially the same effect as increasing the system size.

As observables, we use the number operator N in the CFT basis and the potential energy operators $V(\beta_i)$. Note that N is not a conserved quantity in the DSG. These operators are integrals of local densities, therefore having extensive expectation values in ground or equilibrium states, which makes them suitable for testing the ETH. Given that the unperturbed CFT model is diagonal in terms of Fourier modes, we can compute, as a measure of entanglement in the eigenstates, the Rényi entanglement entropy of one Fourier mode with respect to the rest. In lattice models, the entanglement entropy of an eigenstate computed in the local basis encodes the total correlation between the subsystem in focus and its complement, with localized eigenstates showing low entanglement compared to delocalized ones. Similarly, Fourier space entanglement is low for eigenstates that are "localized" in the Fourier space.

Figure 1 shows numerical results for the expectation values of these quantities in the eigenstates versus their energy. We set $\mu = 0.5$, which corresponds to a good trade-off between remoteness from the perturbative limit and

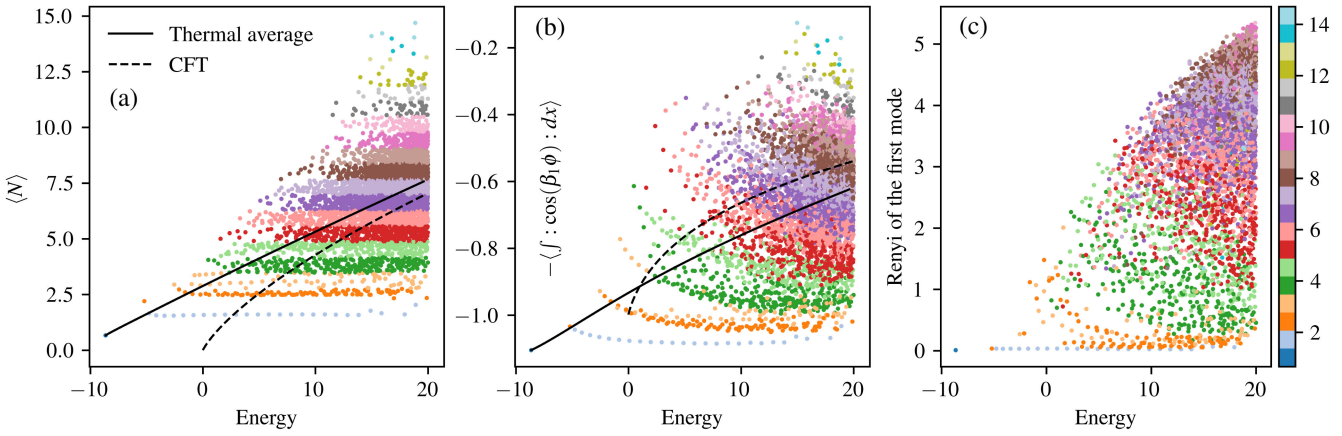

FIG. 1. Eigenstate expectation values of two different observables [(a) particle number N and (b) the cosine potential term $V(\beta_1)$] and (c) of the Rényi entanglement entropy versus the corresponding energy eigenvalues in the units of π/L, for DSG at $\mu = 0.5$ [where $\mu \equiv \lambda(L/\pi)^2$]. The colors indicate the expectation value of particle number N. The black lines are numerically computed thermal curves of expectation values in thermal states of H_{DSG} (full) or H_0 (dashed) versus the corresponding mean thermal energy. These lines are expected to become asymptotically parallel at high energies.

accuracy. While the spectrum exhibits chaotic level spacing statistics, the scatter plots look qualitatively very different from those of chaotic models. In contrast to what the ETH prescribes, the eigenstates span a wide area rather than being concentrated close to the thermal curve, and they are organized in separated families of states, a structure reminiscent of integrable models. In particular, the states with the lowest particle number N form a special family of points located at the edge of the spectra, well aligned along smooth curves spanning the entire energy range, and having almost equidistant energies. These states have very low Fourier space entanglement entropy, which is characteristic of QMBS.

Varying μ from 0 to 1, we observe that some but, as we will see, not all characteristics of this structure are inherited from the perturbative limit. As shown in Fig. 2, in this limit the spectrum is split into vertically aligned and equidistant families of points, and the lowest N eigenstates that look like scars are located at the edge of each family. Given that the unperturbed model is a CFT, its spectrum consists of degenerate energy sectors at equidistant energies with degeneracy numbers increasing rapidly with the energy. A weak perturbation of such a highly degenerate model mixes states predominantly within the same degenerate sector, resulting in decoupled energy spectra. It is, therefore, not surprising that states at the edges of these spectra are less random than in the middle [73]. The above argument provides a generic justification for the emergence of scarlike states in any model that is a weak perturbation of a highly degenerate model with equidistant spectrum. It cannot, however, explain the presence of scars away from the perturbative limit.

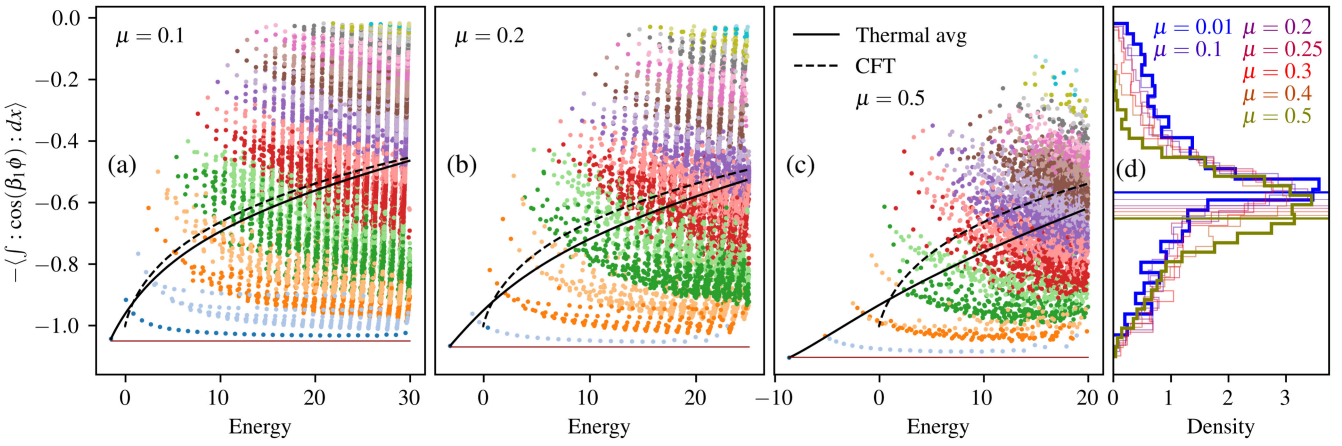

FIG. 2. (a)–(c) The same as in Fig. 1 for a single observable, $V(\beta_1)$, at increasing values of the perturbation strength $\mu \equiv \lambda(L/\pi)^2$. At $\mu = 0.1$, 0.2, and 0.5, there are 28871, 10803, and 5483 converged states, respectively. (d) Histogram of eigenstate expectation values of $V(\beta_1)$ in the energy window $E = 19 \pm 2$ at various μ.

Our numerical results indicate that, in our model, the scar states we observe do not disappear upon increasing μ, which is effectively the same as approaching the thermodynamic limit. Indeed, at $\mu \sim 0.5$, the mixing of the originally decoupled sectors is strong enough that the spectrum is no longer split into gap-separated sectors; nevertheless, scars are still present and aligned along curves that deviate strongly from the thermal average, showing no tendency to approach it (Fig. 2). As shown in Fig. 2(d), focusing on a fixed energy window the density of states close to the bottom edge does not decrease for increasing μ, unlike that of the upper edge, which contracts closer to the thermal average. While we cannot obtain a definite answer to what happens at stronger interaction by means of numerical HT methods, a useful insight into the nature of these states can be gained based on analytical arguments discussed below.

The role of Lorentz symmetry.—Quantum scars may be interpreted as quasiparticle states appearing at unusually high energies. In a general interacting model, low-energy eigenstates can be described as quasiparticles, i.e., collective excitations formed by many real particles moving coordinately under the effect of their mutual interactions. However, at higher energies, quasiparticles typically become unstable due to the large number of possibilities to decay to other quasiparticles, which is why the existence of stable-quasiparticle states at higher energies is surprising.

The spectrum of a typical QFT model admits a quasiparticle description. The ground state is the state that is empty of quasiparticles, and the first excited state contains only one quasiparticle at rest (the lightest of all, if many) with other low-energy states corresponding to moving quasiparticles or more than one quasiparticle scattering with each other. In massive QFT models, eigenstates with finite energy correspond to a finite number of quasiparticles, as there is an energy threshold for the production of massive quasiparticles. For this reason, any eigenstate of a massive QFT can be described by special relativity kinematics for the set of constituent massive quasiparticles.

As a result, signatures of Lorentz invariance are clearly manifested in the structure of QFT spectra on the (P, E) plane, where P and E are the total momentum and energy expectation values, respectively, of the eigenstates. Indeed, for a massive QFT in infinite space with periodic boundary conditions, all excited states are enveloped by the hyperbola $E = \sqrt{P^2 + M^2}$, where the ground state energy is set to zero. In finite-size systems, the spectra are discrete rather than continuous but otherwise exhibit the same characteristics, subject to two types of decaying corrections compared to the infinite-size case [74,75]. Importantly, the above described qualitative structure of the spectrum is valid independently of the interaction strength. Nonperturbative effects at strong interactions are encoded in the complex nature of the quasiparticles (e.g., parameters like mass or charge, scattering amplitudes, etc., depend nontrivially on the interaction),

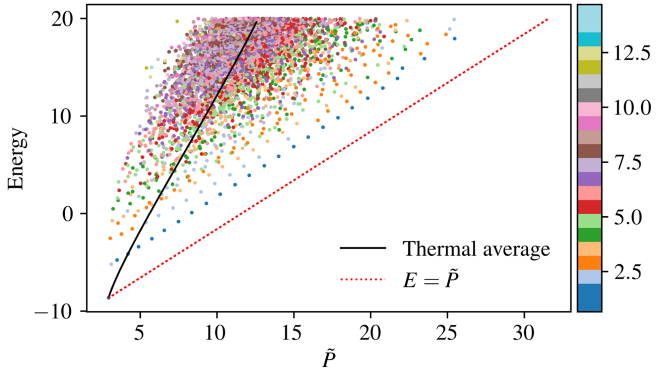

FIG. 3. Scatter plot of $\tilde{P} = \sqrt{\langle P^2 \rangle}$ in each eigenstate versus the corresponding energy eigenvalue E in units of π/L for the numerically computed DSG spectra at $\mu = 0.5$. The colors indicate the particle number expectation value.

whereas qualitative characteristics of the spectra are determined by relativistic kinematical constraints [80].

Tests of the quasiparticle interpretation.—Let us now test the quasiparticle interpretation of the above found scarlike states in DSG, which admits a quasiparticle description [57,61,62]. To check if scarlike states follow the relativistic dispersion relation, it is useful to plot the DSG spectra on the (P, E) plane. For Dirichlet boundary conditions, as in our simulations, the expectation value of the total momentum P in energy eigenstates vanishes [73]; however, the momentum content of a state's quasiparticles can be estimated by measuring P^2. A one-quasiparticle state, for example, corresponds to a standing wave superposition of a quasiparticle moving to both directions with equal and opposite momenta, and $\langle P^2 \rangle$ is proportional to the square of its momentum. Figure 3 shows a scatter plot of $\tilde{P} = \sqrt{\langle P^2 \rangle}$, which is an extensive quantity, versus E, for the numerical DSG spectrum. The QMBS states are prominently aligned parallel to the "light cone" line $E = \tilde{P}$. Interpreted in view of the previous observations, this means that the scarlike states can be identified as one-quasiparticle states of the above theoretical description.

To further validate this interpretation, we investigate the characteristics of scar states and compare with theoretical predictions based on the above. Figure 4 shows the occupation numbers $n(k)$ of the CFT harmonic modes computed in the ground state and scar states of DSG at $\mu = 0.5$. The interacting ground state is significantly different from the CFT vacuum, having occupations that perfectly match those of a "squeezed vacuum" state [73]. Next, we observe that the scar states have approximately the same mode occupations as the ground state except for an additional peak at only one mode each, which is a clear indication that each scar contains a single quasiparticle with different wave numbers. Based on this description of scar states as "squeezed excited states," we can analytically estimate the expectation values of local observables in

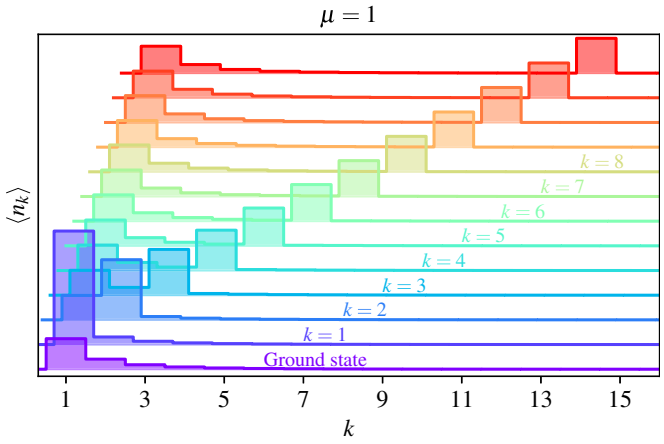

FIG. 4. Occupation numbers $\langle n_k \rangle$ for the lowest few scar states at strong coupling $\mu = 1$.

them. For example, $V(\beta_1)$ is expected to approach a horizontal line for large energies [73], and this is indeed the behavior of scar states as shown in Fig. 2. Note that the thermal line is clearly nonhorizontal at large energies and is, instead, expected to approach the CFT thermal line.

Deviations from the ETH.—Several important conclusions can be drawn from the above interpretation. First, the observed QMBS are nothing but one-quasiparticle states of the interacting QFT model we studied and should be present throughout the entire range of the energy spectrum. Second, they are expected to persist for arbitrary interaction strength beyond the values explored numerically. Third, their property of violating the ETH is guaranteed by the fact that they will always be located far from the bulk of other eigenstates and aligned along curves that diverge from the thermal average line. This is true, because (i) the thermal average line of a local observable in any QFT model that is a perturbation of a CFT by a relevant operator, tends to become parallel to that of the CFT in the high energy limit and (ii) one-quasiparticle states are located along a line determined by relativistic kinematics.

Indeed, the entire spectrum of a relativistic QFT is symmetric under boosts in the thermodynamic limit, and any state of the family of one-quasiparticle states can be brought to the bottom edge of the spectrum by such a boost. Therefore, all states in the vicinity of the hyperbolic line should be considered as the "edge" of the spectrum where nonrandom states can be present. Given that for a general observable these two lines diverge, the above statements, which are expected to hold in the thermodynamic limit, imply that the strong version of the ETH cannot hold, whereas the weak version of the ETH may still be valid. Note, however, that, as shown in Fig. 2(d), the numerically computed density of states close to the QMBS line does not show any tendency to decrease for increasing μ. At the same time, it is not clear if some generalized version of the ETH could hold as a result of Lorentz symmetry: Unlike other symmetries, Lorentz transformations leave the action rather than the Hamiltonian invariant, and the energy spectrum is constrained by the symmetry in a nontrivial way.

Discussion.—Clearly, the above scenario suggests a strong distinction between lattice models and QFT. Perturbing a free lattice model by a generic interaction would not give rise to such atypical eigenstates, because one-quasiparticle states are limited to a finite energy range close to the ground state. On the contrary, in QFT, Lorentz invariance, which is exactly valid in the thermodynamic limit, imposes strong kinematical constraints on the spectrum at all energy scales. Motivated by the above arguments based on RG theory and on Lorentz symmetry, we expect that analogous deviations from the ETH hold in any relativistic nonintegrable QFT that admits a quasiparticle description.

We thank Per Moosavi, Alexios Michailidis, Elias Kiritsis, and Gabor Takacs for useful discussions. We thank the support of the HPCaVe computational platform of Sorbonne University, where the main part of the computation has been performed. M. S. is grateful for the environment provided by ISCD and the resources received during his Ph.D. under the supervision of M. Casula and R. Vuilleumier. S. S. acknowledges support by the European Union's Horizon 2020 research and innovation program under the Marie Skłodowska-Curie Grant Agreement No. 101030988. T. P. acknowledges support from the Program P1-0402 of Slovenian Research Agency (ARRS).

*miha.srdinsek@upmc.fr

[1] J. M. Deutsch, Phys. Rev. A **43**, 2046 (1991).
[2] M. Srednicki, Phys. Rev. E **50**, 888 (1994).
[3] M. Rigol, V. Dunjko, and M. Olshanii, Nature (London) **452**, 854 (2008).
[4] P. Reimann, New J. Phys. **17**, 055025 (2015).
[5] L. D'Alessio, Y. Kafri, A. Polkovnikov, and M. Rigol, Adv. Phys. **65**, 239 (2016).
[6] J. M. Deutsch, Rep. Prog. Phys. **81**, 082001 (2018).
[7] R. Nandkishore and D. A. Huse, Annu. Rev. Condens. Matter Phys. **6**, 15 (2015).
[8] L. F. Santos and M. Rigol, Phys. Rev. E **81**, 036206 (2010).
[9] W. Beugeling, R. Moessner, and M. Haque, Phys. Rev. E **89**, 042112 (2014).
[10] F. Borgonovi, F. Izrailev, L. Santos, and V. Zelevinsky, Phys. Rep. **626**, 1 (2016).
[11] L. Foini and J. Kurchan, Phys. Rev. E **99**, 042139 (2019).
[12] C. J. Turner, A. A. Michailidis, D. A. Abanin, M. Serbyn, and Z. Papić, Nat. Phys. **14**, 745 (2018).
[13] C. J. Turner, A. A. Michailidis, D. A. Abanin, M. Serbyn, and Z. Papić, Phys. Rev. B **98**, 155134 (2018).
[14] C.-J. Lin and O. I. Motrunich, Phys. Rev. Lett. **122**, 173401 (2019).

[15] S. Choi, C. J. Turner, H. Pichler, W. W. Ho, A. A. Michailidis, Z. Papić, M. Serbyn, M. D. Lukin, and D. A. Abanin, Phys. Rev. Lett. **122**, 220603 (2019).
[16] W. W. Ho, S. Choi, H. Pichler, and M. D. Lukin, Phys. Rev. Lett. **122**, 040603 (2019).
[17] K. Bull, I. Martin, and Z. Papić, Phys. Rev. Lett. **123**, 030601 (2019).
[18] K. Bull, J.-Y. Desaules, and Z. Papić, Phys. Rev. B **101**, 165139 (2020).
[19] M. Schecter and T. Iadecola, Phys. Rev. Lett. **123**, 147201 (2019).
[20] A. A. Michailidis, C. J. Turner, Z. Papić, D. A. Abanin, and M. Serbyn, Phys. Rev. X **10**, 011055 (2020).
[21] S. Moudgalya, S. Rachel, B. A. Bernevig, and N. Regnault, Phys. Rev. B **98**, 235155 (2018).
[22] S. Moudgalya, N. Regnault, and B. A. Bernevig, Phys. Rev. B **98**, 235156 (2018).
[23] T. Iadecola and M. Schecter, Phys. Rev. B **101**, 024306 (2020).
[24] D. K. Mark, C.-J. Lin, and O. I. Motrunich, Phys. Rev. B **101**, 195131 (2020).
[25] S. Chattopadhyay, H. Pichler, M. D. Lukin, and W. W. Ho, Phys. Rev. B **101**, 174308 (2020).
[26] N. O'Dea, F. Burnell, A. Chandran, and V. Khemani, Phys. Rev. Res. **2**, 043305 (2020).
[27] K. Pakrouski, P. N. Pallegar, F. K. Popov, and I. R. Klebanov, Phys. Rev. Lett. **125**, 230602 (2020).
[28] J. Ren, C. Liang, and C. Fang, Phys. Rev. Lett. **126**, 120604 (2021).
[29] C. M. Langlett, Z.-C. Yang, J. Wildeboer, A. V. Gorshkov, T. Iadecola, and S. Xu, Phys. Rev. B **105**, L060301 (2022).
[30] A. Chandran, T. Iadecola, V. Khemani, and R. Moessner, Annu. Rev. Condens. Matter Phys. **14**, 443 (2023).
[31] G. Biroli, C. Kollath, and A. M. Läuchli, Phys. Rev. Lett. **105**, 250401 (2010).
[32] J. Cardy, Phys. Rev. Lett. **112**, 220401 (2014).
[33] P. Basu, D. Das, S. Datta, and S. Pal, Phys. Rev. E **96**, 022149 (2017).
[34] S. Datta, P. Kraus, and B. Michel, J. High Energy Phys. 07 (2019) 143.
[35] S. He, F.-L. Lin, and J.-j. Zhang, J. High Energy Phys. 08 (2017) 126.
[36] N. Lashkari, A. Dymarsky, and H. Liu, J. Stat. Mech. (2018) 033101.
[37] A. Dymarsky and K. Pavlenko, Phys. Rev. Lett. **123**, 111602 (2019).
[38] K. Goto, A. Mollabashi, M. Nozaki, K. Tamaoka, and M. T. Tan, J. High Energy Phys. 06 (2022) 100.
[39] Z. Yao, L. Pan, S. Liu, and H. Zhai, Phys. Rev. B **105**, 125123 (2022).
[40] A. L. Fitzpatrick, J. Kaplan, M. T. Walters, and J. Wang, J. High Energy Phys. 09 (2015) 019.
[41] C. T. Asplund, A. Bernamonti, F. Galli, and T. Hartman, J. High Energy Phys. 02 (2015) 171.
[42] T. Anous, T. Hartman, A. Rovai, and J. Sonner, J. High Energy Phys. 07 (2016) 123.
[43] C. T. Asplund, A. Bernamonti, F. Galli, and T. Hartman, J. High Energy Phys. 09 (2015) 110.
[44] G. J. Turiaci and H. Verlinde, J. High Energy Phys. 12 (2016) 110.
[45] Y. Kusuki, J. High Energy Phys. 01 (2019) 025.
[46] J. Kudler-Flam, Y. Kusuki, and S. Ryu, J. High Energy Phys. 04 (2020) 074.
[47] J. Kudler-Flam, Y. Kusuki, and S. Ryu, J. High Energy Phys. 03 (2021) 146.
[48] J.-Y. Desaules, D. Banerjee, A. Hudomal, Z. Papidć, A. Sen, and J. C. Halimeh, Phys. Rev. B **107**, L201105 (2023).
[49] J.-Y. Desaules, A. Hudomal, D. Banerjee, A. Sen, Z. Papić, and J. C. Halimeh, Phys. Rev. B **107**, 205112 (2023).
[50] N. J. Robinson, A. J. A. James, and R. M. Konik, Phys. Rev. B **99**, 195108 (2019).
[51] M. Srdinšek, Master's thesis, University of Ljubljana, Faculty of Mathematics and Physics, 2020.
[52] L. V. Delacrétaz, A. L. Fitzpatrick, E. Katz, and M. T. Walters, J. High Energy Phys. 02 (2023) 045.
[53] M. Srdinsek, T. Prosen, and S. Sotiriadis, Phys. Rev. Lett. **126**, 121602 (2021).
[54] M. Kormos, M. Collura, G. Takács, and P. Calabrese, Nat. Phys. **13**, 246 (2017).
[55] R. M. Konik and Y. Adamov, Phys. Rev. Lett. **98**, 147205 (2007).
[56] M. Hogervorst, S. Rychkov, and B. C. van Rees, Phys. Rev. D **91**, 025005 (2015).
[57] G. Delfino and G. Mussardo, Nucl. Phys. **B516**, 675 (1998).
[58] Z. Bajnok, L. Palla, G. Takács, and F. Wágner, Nucl. Phys. **B587**, 585 (2000).
[59] Z. Bajnok, L. Palla, G. Takács, and F. Wágner, Nucl. Phys. **B601**, 503 (2001).
[60] G. Z. Tóth, J. Phys. A **37**, 9631 (2004).
[61] G. Takács and F. Wágner, Nucl. Phys. **B741**, 353 (2006).
[62] G. Mussardo, V. Riva, and G. Sotkov, Nucl. Phys. **B687**, 189 (2004).
[63] A. Roy and S. L. Lukyanov, Nat. Commun. **14**, 7433 (2023).
[64] V. P. Yurov and A. B. Zamolodchikov, Int. J. Mod. Phys. A **05**, 3221 (1990).
[65] V. P. Yurov and A. B. Zamolodchikov, Int. J. Mod. Phys. A **06**, 4557 (1991).
[66] I. Kukuljan, S. Sotiriadis, and G. Takács, Phys. Rev. Lett. **121**, 110402 (2018).
[67] I. Kukuljan, S. Sotiriadis, and G. Takács, J. High Energy Phys. 07 (2020) 224.
[68] I. Kukuljan, Phys. Rev. D **104**, L021702 (2021).
[69] P. Emonts and I. Kukuljan, Phys. Rev. Res. **4**, 033039 (2022).
[70] D. Horváth, K. Hódsági, and G. Takács, Comput. Phys. Commun. **277**, 108376 (2022).
[71] D. X. Horváth, S. Sotiriadis, M. Kormos, and G. Takács, SciPost Phys. **12**, 144 (2022).
[72] In DSG, convergence is relatively fast compared to polynomial interactions (e.g., the ϕ^4 model), because the scaling dimension of the cosine operator, which is $\Delta = \beta^2/(4\pi)$, can be chosen arbitrarily small.
[73] See Supplemental Material at http://link.aps.org/supplemental/10.1103/PhysRevLett.132.021601 for additional details about the perturbative argument for the presence of scarlike states at weak interaction, the constraints of relativistic kinematics on the QFT spectrum, the

construction of the total momentum operator for Dirichlet boundary conditions, the derivation of the observable expectation values in thermal states, and the analysis of observable expectation values in one-quasiparticle eigenstates. Supplemental Material includes Refs. [53,61,71,74–79].

[74] M. Lüscher, Commun. Math. Phys. **104**, 177 (1986).

[75] M. Lüscher, Commun. Math. Phys. **105**, 153 (1986).

[76] D. Szász-Schagrin, B. Pozsgay, and G. Takács, SciPost Phys. **11**, 037 (2021).

[77] I. Albrecht, J. Herrmann, A. Mariani, U.-J. Wiese, and V. Wyss, Ann. Phys. (Amsterdam) **452**, 169289 (2023).

[78] G. Feverati, F. Ravanini, and G. Takács, Phys. Lett. B **430**, 264 (1998).

[79] Z. Bajnok, L. Palla, G. Takács, and F. Wágner, Nucl. Phys. **B601**, 503 (2001).

[80] R. Eden, R. Eden, P. Landshoff, D. Olive, and J. Polkinghorne, *The Analytic S-Matrix* (Cambridge University Press, Cambridge, England, 2002).